SAND2017-12996C

3D PARTICLE TRACKING FROM PERSPECTIVE-SHIFTED PLENOPTIC IMAGES

Elise Munz Hall[1,2], Daniel R. Guildenbecher[2], and Brian S. Thurow[1]

[1]Department of Aerospace Engineering, Auburn University, Auburn, Alabama 36849, USA
[2]Sandia National Laboratories, Albuquerque, New Mexico 87185, USA

ABSTRACT

3D particle tracking methods have previously been developed using the refocusing capabilities of plenoptic imaging due to the straightforward nature of refocused images as a volumetric representation of a particle field. This work develops an algorithm to determine 3D particle position by exploiting the perspective-shift capabilities of the plenoptic camera. This algorithm is validated using an experimental data set previously examined in a refocusing based particle location study in which a static particle field is translated known distances. Preliminary results suggest similar uncertainty measurements are obtained using the newly developed algorithm at significantly reduced computational costs. The final work will include refinements in outlier detection and overlapping particle measurements as well as examination of experimental configurations in which the magnification and imaging distance are varied.

1. INTRODUCTION

Plenoptic imaging is an implementation of light field imaging in which spatial multiplexing by means of a microlens array is used to encode a 4D light field onto a 2D sensor plane, thus capturing both the spatial and angular information defining the light rays emanating from a scene. This allows for the creation of a 3D representation of a scene from a single snapshot. Though this concept originated over a century ago, described as integral photography by Lippmann [1], practical implementations of plenoptic cameras are a more recent development linked to the availability of high resolution digital image sensors and computational capability increases. Adelson and Wang presented the first implementation of a plenoptic camera in 1992 [2], and Ng. et al created a handheld version in 2005 [3]. Since these early implementations, the development and use of this technology has greatly increased and plenoptic cameras have been applied to a wide variety of scientific applications including many implementations of volumetric particle based imaging techniques [4–9].

Previously, the refocusing capability of plenoptic imaging has been exploited to determine particle positions from a series of computationally refocused images and metrics of uncertainty and computational efficiency have been obtained [10]. The use of refocused images to obtain particle locations is perhaps the most obvious use of plenoptic data for particle location; however, plenoptic data can also be used to create perspective-shifted images. In this work, an algorithm is developed to exploit the perspective-shift capability of plenoptic imaging to determine 3D particle positions. This algorithm is applied to the same data set used in Hall et al [10] to compare the uncertainty characteristics and efficiency of this algorithm to the previously implemented refocusing based technique.

2. BACKGROUND AND PREVIOUS WORK

The plenoptic camera implementation discussed in this work uses a standard scientific camera that is modified by the insertion of a microlens array placed between the main lens and the image sensor. These microlenses redirect

incoming light rays to different image sensor locations according to angle of propagation, resulting in an instantaneous image that contains volumetric information. Each microlens creates a sub-aperture image of the main lens aperture as shown in Figure 1 where a raw plenoptic image is shown on the left. This is an image of a simulated particle field. Straight pins are used to represent static particles to allow for uncertainty analysis. The following inset images demonstrate the sub-aperture images that simultaneously encode spatial and angular information. For convenience, a two-plane parameterization is used to fully define the light ray locations in space where (u,v) defines coordinates on the main lens aperture and (s,t) defines coordinates on the microlens plane, again shown in Figure 1. The light field, which defines the amount of light travelling in all directions through all points in space, is a function of these four coordinates, $L(u,v,s,t)$. In post-processing this additional information can be used to create volumetric representations of the scene by computationally changing the depth of the focal plane or the angle from which the scene is viewed. These are termed refocused and perspective-view images respectively and each contain information that can be used to identify particle position in 3D space. These computationally created images are defined by the relationship between the light field and the synthetic light field, L' [3],

$$L'(u,v,s',t') = L\left(u,v,u+\frac{s'-u}{\alpha},v+\frac{t'-v}{\alpha}\right), \tag{1}$$

where α is a scalar value that relates the distance between the aperture plane and image sensor plane, l_i, to the distance between the aperture plane and virtual image sensor plane l_i', also shown in Figure 1.

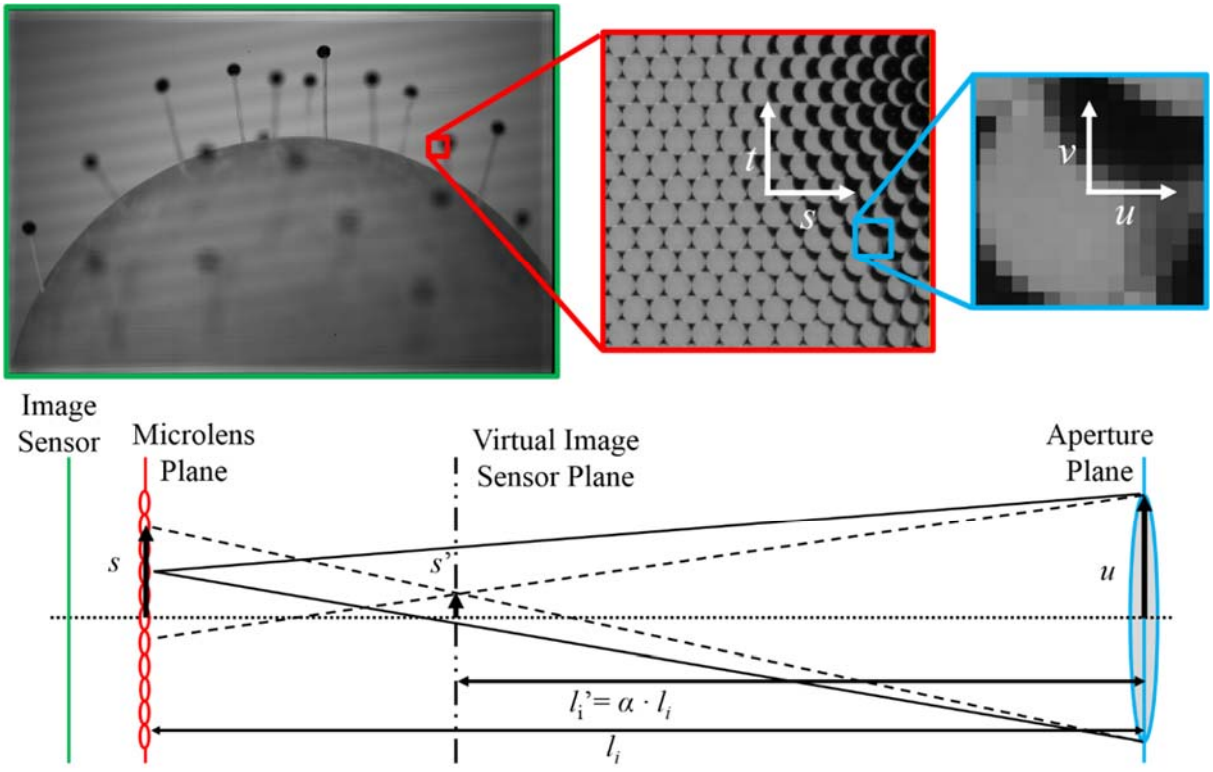

Figure 1. *Raw image and insets corresponding to the two-plane parameterization (top) and schematic depicting the elements of plenoptic imaging (bottom).*

A. Refocusing

Computationally changing the depth at which the image is focused is achieved by integrating Eq. (1) over the sub-aperture images as,

$$E(s',t') = \iint L\left(u, v, u + \frac{s'-u}{\alpha}, v + \frac{t'-v}{\alpha}\right) du dv, \tag{2}$$

where the refocused depth is determined by α, and $E(s',t')$ represents the refocused image. Figure 2 demonstrates an example where the raw image from Figure 1 is refocused to two different depths, which can be seen in comparing which particles appear in focus in each image. Creating refocused images at a variety of depths in this manner produces a conceptually straightforward method of a volumetric representation of a scene, which is called a focal stack. In previous works [6,10,11], focal stacks with many slices were used to determine 3D locations of particles using a modified version of the hybrid particle detection method based on minimum intensity and maximum edge sharpness which was originally developed for holography [12]. Due to the requirements of integration over all pixels behind each microlens and using a sufficient number of depth planes, the creation of these focal stacks is a computationally expensive process.

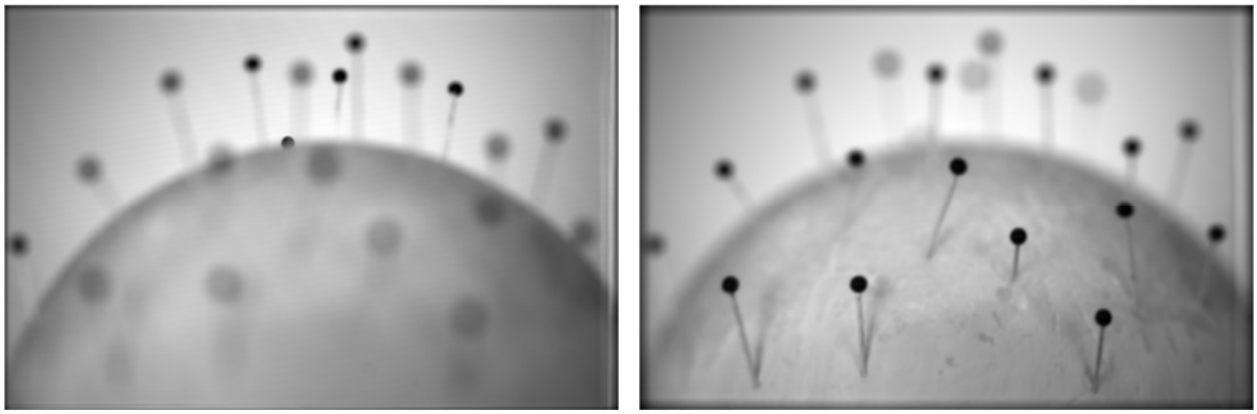

Figure 2. *Example of refocusing capability, an image focused farther from (left) and nearer to (right) the camera than the nominal focal plane.*

B. Perspective-shift

Creating a perspective-shifted image can be described as combining the pixel from behind the same aperture location relative to each microlens and is mathematically defined by,

$$E(s,t) = L\left(u_0, v_0, s, t\right), \tag{3}$$

where (u_0,v_0) is the selected aperture location. As compared to refocusing, the creation of perspective views is mathematically simpler and therefore implementation requires significantly less computational resources. An example of a perspective-shift is shown in Figure 3 where the raw image from Figure 1 was shifted to the left and right. The shift is most evident in comparing the relative distance between objects as noted in the colored ovals. The relative location of an object in different perspective-views provides an indication of the location of the objects in 3D space,

though in a less obvious manner than in determining depth from focus. This is similar to the method used in stereo imaging. In plenoptic imaging, many more than two views are available and can be combined to produce a single measurement of 3D particle location.

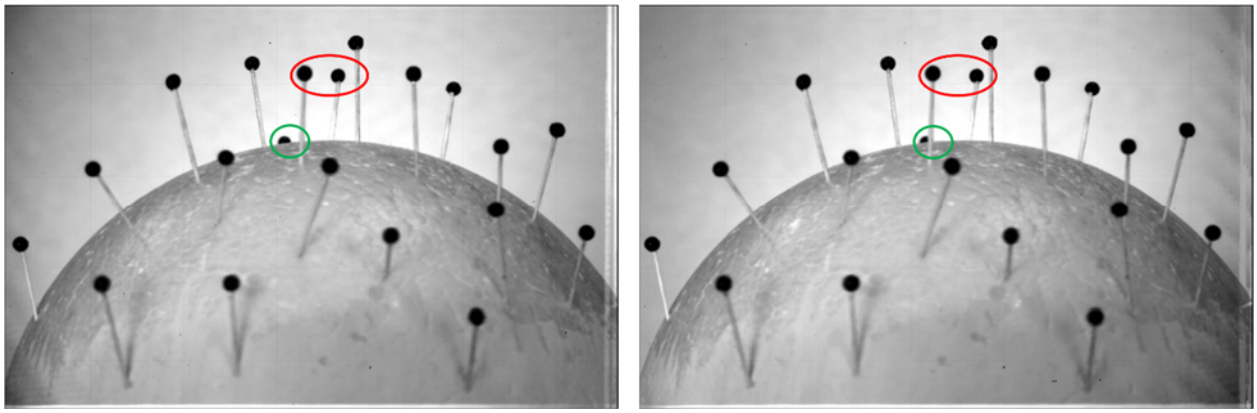

Figure 3. *Example of perspective-shift capability, an image shifted to the left (left) and right (right).*

3. ALGORITHM DEVELOPMENT

The algorithm developed in this work uses the apparent discrepancy in 2D particle locations between different perspective views to determine 3D particle locations. This method is conceptually similar to those used in stereo imaging except that many more views are used, which provides redundancy and allows erroneous measurements to be identified and removed without removing an entire particle measurement. To account for lens distortions and other experimental error, the Direct Light Field Calibration (DLFC) is applied in the determination of object space particle locations. Creation of the calibration coefficients required for DLFC is based on a range of dot cards with known physical dimensions as described in Hall et al [11]. Here, a 4th order polynomial fit is used rather than a 3rd order as was done in [11]. This increase in order was executed because in application of a 3rd order fit, a distinct systematic warping was still present in the resulting data as indicated by measurement of particle locations in dot card images. Application of a 4th order fit, which required 126 coefficients in each dimension, removed this systematic error. This calibration is created only once for a given experimental condition. This results in a modification of the perspective-shift equation where Eq. (3) becomes,

$$E(s,t) = L\left(u_0, v_0, P_s\left(Y,Y,Z,u,v\right), P_t\left(Y,Y,Z,u,v\right)\right). \tag{4}$$

The actual data processing segment of the algorithm begins with the creation of a range of perspective-shifted images from a single raw image. To avoid edge effects, only 49 views corresponding to 49 (u,v) locations are currently used. Particle locations are measured in each of these views using standard MATLAB region finding tools. The sets of particle locations from individual views are then grouped by particle. This results in a set of (s,t,u,v) locations for each particle. These measured locations for each particle are used to determine the (x,y,z) object space particle location by applying a MATLAB nonlinear least squares solver which minimizes the results of application of DLFC and the measured (s,t,u,v) locations.

4. PRELIMINARY EXPERIMENTAL RESULTS

The accuracy and precision of particle location measurements achievable using the method developed in this work is assessed using the experimental data set examined in Hall et al [10] in which a rigid particle field is simulated by straight pin heads inserted at random orientations into a foam ball as shown in Figure 4. The particle field is mounted on a translation stage allowing precisely known displacements along the optical depth direction, z.

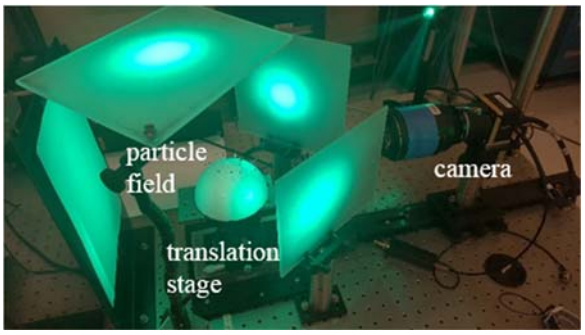

Figure 4. *Experimental configuration including simulated particle field, translation stage, and plenoptic camera.* [10]

Data was collected at four different magnifications and three different distances from the particle field resulting in 12 configurations to allow examination of trends based on field of view and object distance. In each of these configurations, the particle field was translated in 1 mm increments along the entire 50 mm travel distance of the translation stage and images were captured at each position. This process was repeated 50 times for each configuration to achieve a large statistically significant data set. Further experimental details can be found in Hall et al [10].

The configuration with a magnification of 0.5 and the center distance between the camera and the particle field has been processed using the algorithm developed in this work and provides preliminary indications of the achievable uncertainty. All of the error measurements determined from this data set are shown in Figure 5, which demonstrates that the errors appear to be normally distributed. The number of measurements available and the general scale of errors is also evident from this plot and appears similar to those achieved with the previously obtained uncertainties [10].

To allow comparison of these error measurements to those previously obtained in Hall et al [10], accuracy and precision were examined as a function of depth. Figure 6 displays the accuracy as a function of depth determined using the method developed here as well as the results from Hall et al [10] for this configuration. Figure 6a displays the errors in physical coordinates while Figure 6b normalizes the z position by the near and far limits of the depth of field and the error by the pitch of a microlens in object space, Δx. Both methods show similar errors and trends for this configuration. Figure 7 displays similar plots for precision, in which case the two methods differ more significantly with the newly developed algorithm resulting in lower precision at the depths closer to the camera and better precision farther from the camera. Given that the accuracy of these measurements is relatively similar, the lower precision is likely the result of outliers in the measurements and can be improved with continued refinement of the perspective view algorithm.

The computational requirements of the perspective view algorithm developed here provides a significant advantage over previous refocusing based methods. Measurement of particle positions from a single image

parallelized in MATLAB on a 12 core desktop computer requires about an hour using depth from refocusing methods and just under a minute using the perspective shift based method developed here – a decrease of approximately two orders of magnitude. Considering the similar measurement uncertainties achieved using each method, this speed up is particularly significant.

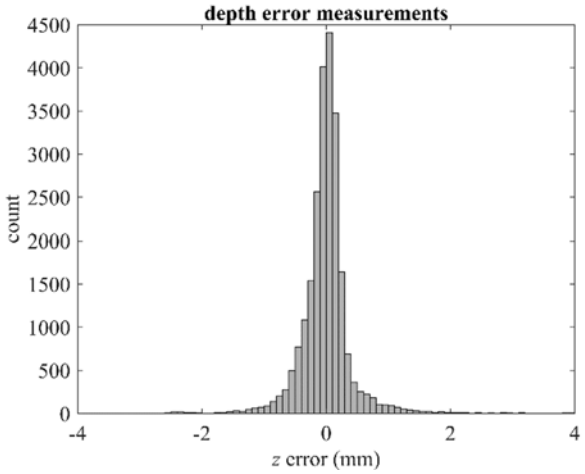

Figure 5. *Histogram of the errors measured from the middle configuration with a magnification of 0.5.*

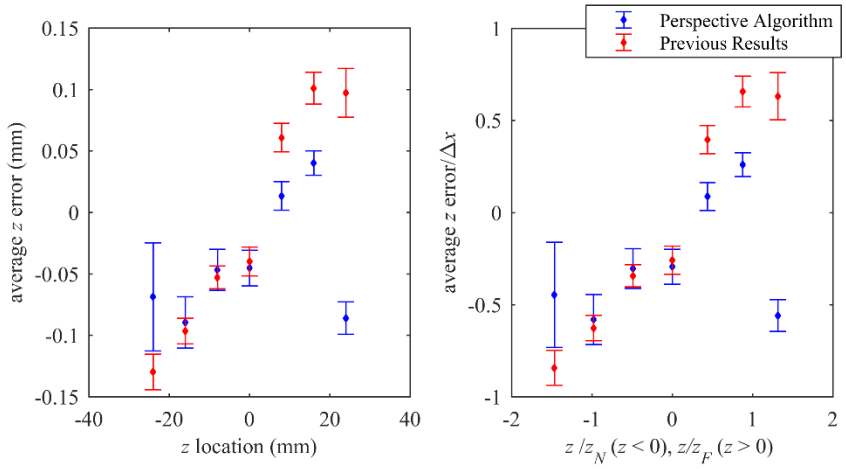

Figure 6. *Average depth error as a function of particle depth, z, in physical dimensions (a) and normalized (b).*

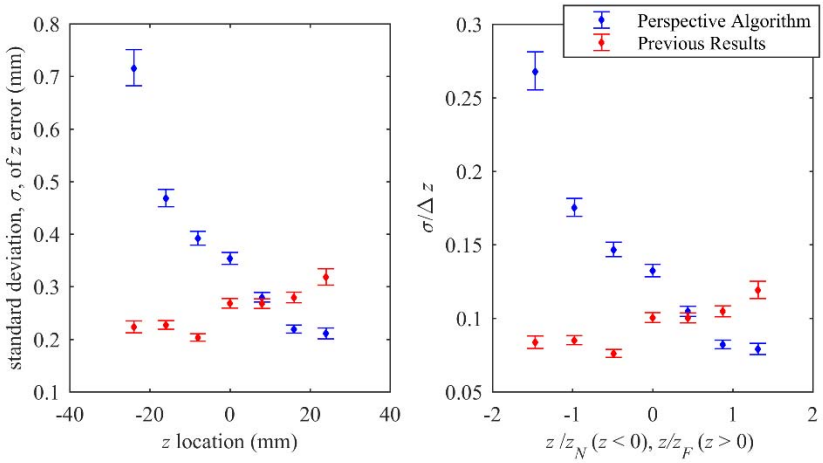

(a) (b)

Figure 7. *Standard deviation of depth error as a function of particle depth, z, in physical dimensions (a) and normalized (b).*

5. REMAINING WORK

A variety of topics will be addressed in refinement of the perspective-shift based particle location algorithm developed in this work. First, the current implementation relies on a relatively sparse particle field and does not account for particles that overlap in the in-plane dimensions. This can result in significant errors when measurements from multiple particles are identified as a single particle. Attempts to mitigate this issue will be explored including rejection of particle locations that vary too significantly between perspective views and refinement of particle matching requirements. Second, the MATLAB nonlinear least squares solver is currently being used with generally default settings, more work will be done to examine the effect of these settings on particle location accuracy. Attempts will be made to select more appropriate settings, though early attempts at varying these settings have shown that the solver results are robust to changes in input for the scope of these problems, but may affect the convergence rate. Third, only the 49 perspective views closest to the center of the aperture are currently used to determine particle positions as portions of the remaining views display dark regions due to vignetting. Allowing rejection of these regions will allow for the use of portions of these views and increase the number of views used to measure particle location.

This refined algorithm will be used to process the entire data set analyzed in Hall et al [10] to determine trends in measurement uncertainty based on magnification and volume location which can be compared to those determined in that work.

FUNDING INFORMATION

Sandia National Laboratories is a multi-mission laboratory managed and operated by National Technology and Engineering Solutions of Sandia LLC, a wholly owned subsidiary of Honeywell International Inc. for the U.S. Department of Energy's National Nuclear Security Administration under contract DE-NA0003525.

REFERENCES

1. G. Lippmann, "La photographie integrale," Comptes-Rendus, Acad. des Sci. **146**, 446–551 (1908).

2. E. H. Adelson and J. Y. A. Wang, "Single lens stereo with a plenoptic camera," IEEE Trans. Pattern Anal. Mach. Intell. **14**, 99–106 (1992).

3. R. Ng, M. Levoy, G. Duval, M. Horowitz, and P. Hanrahan, "Light field photography with a hand-held plenoptic camera," Stanford Tech Rep. CTSR 1–11 (2005).

4. T. W. Fahringer, K. P. Lynch, and B. S. Thurow, "Volumetric particle image velocimetry with a single plenoptic camera," Meas. Sci. Technol. **26**, 115201 (2015).

5. H. Chen and V. Sick, "Three-dimensional three-component air flow visualization in a steady-state engine flow bench using a plenoptic camera," SAE Int. J. Engines **10**, 625–635 (2017).

6. E. M. Hall, B. S. Thurow, and D. R. Guildenbecher, "Comparison of three-dimensional particle tracking and sizing using plenoptic imaging and digital in-line holography," Appl. Opt. **55**, 6410–6420 (2016).

7. H. Chen, V. Sick, M. A. Woodward, and D. Burke, "Human iris 3D imaging using a micro-plenoptic camera," Opt. Life Sci. **2017**, 8–10 (2017).

8. K. C. Johnson, B. S. Thurow, T. Kim, G. Blois, and K. T. Christiansen, "Volumetric velocity measurements in the wake of a hemispherical roughness element," AIAA J. **55**, 2158–2173 (2017).

9. T. T. Truscott, J. Belden, R. Ni, J. Pendlebury, and B. McEwen, "Three-dimensional microscopic light field particle image velocimetry," Exp. Fluids **58**, 16 (2017).

10. E. M. Hall, D. R. Guildenbecher, and B. S. Thurow, "Uncertainty characterization of particle location from refocused plenoptic images," Opt. Express **25**, 21801–21814 (2017).

11. E. M. Hall, T. W. Fahringer, and B. S. Thurow, "Volumetric calibration of a plenoptic camera," AIAA SciTech Forum, 55th Annu. Aerosp. Sci. Meet. 1–13 (2017).

12. D. R. Guildenbecher, J. Gao, P. L. Reu, and J. Chen, "Digital holography simulations and experiments to quantify the accuracy of 3D particle location and 2D sizing using a proposed hybrid method," Appl. Opt. **52**, 3791–3801 (2013).